Supporting Information

Barua et al. 10.1073/pnas.1216893110

SI Text

1. Particle Preparation and Adsorption/Desorption of Proteins from Nanoparticles. Briefly, spherical polystyrene particles were added to a polyvinyl alcohol (PVA) solution, and the film was prepared by air drying. A piece of the film was mounted on the custom-made 1D or 2D stretcher and elongated in mineral oil at 120 °C. After stretching, the film was washed to remove residual oil and dissolved in ice-cold deionized water. The stretched particles were collected by centrifugation, followed by washing five times with ice-cold deionized water to remove residual PVA. Scanning electron microscope (SEM) images of the particles were taken after coating particles with palladium (Hummer 6.2 Sputtering System; Anatech Ltd.) using a Sirion 400 SEM (FEI Co.) at an acceleration voltage of 3 eV. The sizes of at least 30 particles were measured manually using ImageJ software (National Institutes of Health).

Trastuzumab and bovine serum albumin (BSA) were coated on the particle surface by an adsorption method. In detail, particles were centrifuged at 14,000 × *g* for 30 min, washed using Tris·HCl buffer (pH 8.5), and dispersed in 1 mL of the same buffer. A 500-μL solution of 0.2 mg/mL trastuzumab (isoelectric point = 8.45) and BSA (isoelectric point = 4.7) was prepared in Tris·HCl buffer and sodium acetate buffer (pH 4.8), respectively, which had ionic strengths close to the isoelectric points of the antibodies. The particles were added to the antibody solutions and allowed to mix for 2 h at room temperature. The unbound antibodies were separated from the antibody-coated polystyrene particles by centrifugation. The unbound free antibodies in the three supernatants collected were quantified using a Pierce Micro BCA protein kit (Thermo Scientific). The amount of adsorbed antibodies was calculated by subtracting the free antibodies in the supernatants from the original amount added. The antibody-coated particles were washed twice using phosphate-buffer saline (PBS), stored at 4 °C, and used for experiments within 24 h.

The desorption kinetics of adsorbed antibody were studied at 0, 0.5, 2, and 24 h in PBS buffer and 10% fetal bovine serum (FBS) containing PBS at 37 °C. The nanoparticle suspension was centrifuged at different times to collect the free antibody in the supernatant. The amount of trastuzumab or BSA desorbed in PBS was quantified using the Pierce Micro BCA assay (Thermo Scientific). To measure desorption of the antibody in the presence of FBS, trastuzumab antibody was conjugated to a red fluorescent dye, Alexa 594 (Invitrogen). Alexa 594–conjugated BSA (Invitrogen) was used as a control. The fluorescence intensity of Alexa 594–conjugated trastuzumab and BSA in the supernatants of 10% FBS–PBS was measured using 590/617 excitation/emission filters of a plate reader (Tecan). The background fluorescence of 10% FBS–PBS was subtracted. Results were expressed as a percentage of the total fluorescence intensity of Alexa 594–conjugated antibody in 10% FBS–PBS and plotted as a function of time.

2. Preparation and Characterization of Trastuzumab-Coated Camptothecin Nanorods. Camptothecin nanorods were prepared from camptothecin (Sigma-Aldrich) solution in dimethylsulfoxide (DMSO; Fisher) by the solvent diffusion method. Briefly, 2.5 mL camptothecin (CPT) solution of 10 mg/mL in DMSO was injected using a syringe pump (KD Scientific Inc.) into 50 mL of 1% polyvinyl alcohol (PVA; 13–23 kDa; Sigma-Aldrich) surfactant. The final concentration of DMSO in 1% PVA/water mixture was 0.05%. The camptothecin dispersion was stirred at 300 rpm using a stirrer plate (Thermo Scientific) at room temperature (22 °C). Nanorods were formed at the boundary where DMSO diffused slowly into water. Nanorods were separated from the dispersion by centrifuging at 11,000 × *g* for 1 h and washed with water five times. Camptothecin concentrations were measured by reading absorbance at 366 nm using a spectrophotometer (Tecan Safire) and camptothecin calibration curves. Camptothecin nanorods were stored in water at 4 °C until further use. Physicochemical characterizations such as size and zeta potential of camptothecin were measured using scanning electron microscopy and dynamic light scattering, respectively. For active targeting of human epidermal growth factor receptor 2 positive ($HER2^+$) breast cancer cells, trastuzumab was adsorbed to camptothecin nanorods, and unbound antibody was measured using a Pierce Micro BCA assay kit (Thermo Scientific). The adsorption efficiency was calculated by subtracting unbound antibody from the initial antibody. BSA protein was used as a negative control. The results are shown in Table S1. Zeta potentials of camptothecin and trastuzumab-coated camptothecin are shown in Table S3.

3. Effects of Trastuzumab-Coated Camptothecin Nanorods on Breast Cancer Cell Growth in Vitro. The efficacy of trastuzumab-coated camptothecin was evaluated in BT-474, SK-BR-3, and MDA-MB-231 breast cancer cell lines in vitro. The controls used in this experiment were as follows: BSA-coated camptothecin and trastuzumab alone in PBS. Cells were seeded in 96-well plates (8,400 per well) and treated with trastuzumab-coated camptothecin nanorods and the controls for 2 h, with a final camptothecin dose of 0.1 μg/mL The medium was removed after 2 h of incubation. Cells were incubated further for 94 h in freshly added medium. Total number of live cells was quantified using a live/dead assay kit (Invitrogen). The percentage inhibition in cell proliferation was calculated based on the PBS-treated controls and using the following equation:

$$100 * \left(\frac{Number\ of\ cells\ in\ (PBS\ treated\ control - camptothecin\ or\ trastuzumab\ treated\ cells)}{Number\ of\ cells\ in\ PBS\ treated\ control} \right).$$

4. Fabrication of Poly(Lactide-Coglycolic Acid) Nanorods. Poly(lactide-coglycolic acid) (PLGA) nanospheres were prepared by a solvent diffusion method. Briefly, 200 mg of PLGA was dissolved in 20 mL of acetone, and the PLGA solution was added to 1.0% (wt/vol) PVA through a syringe pump at a rate of 20 mL/h under stirring, followed by 24 h of stirring to remove residual organic solvent. The nanospheres produced were collected by centrifugation at 11, 000 × *g* for 1 h and washed three times using double-distilled water. Nanorods were prepared from the nanospheres using the previously published film-stretching method. Briefly, a 10% solution of cold water–soluble PVA (molecular weight,

40–70 kDa; Sigma-Aldrich) was prepared in water with 2% (wt/vol) glycerol. The nanospheres were added to this mixture, and the mixture was casted on a flat surface. After a drying process at room temperature, the film was cut into sections and mounted on axial stretchers. The films were stretched in mineral oil at 60 °C and air dried for 10 h. After residual oil was removed using isopropanol, the film was dissolved in ice-cold deionized water and nanorods were collected by centrifuging at 11,000 × g for 1 h, followed by washing five times with ice-cold deionized water to remove residual PVA.

5. Mechanisms of Shape-Dependent Nanoparticle Interactions. Although the studies presented here suggest that enhanced uptake of nanorods can be explained by enhanced surface binding, additional factors associated with multivalent interactions and particle morphology likely also play a role in the interplay between particle shape and surface chemistry (1, 2). Studies have reported that it is thermodynamically favorable to wrap the cell membrane around a rod than a sphere because the mean curvature radius of a rod is half that of the corresponding sphere, resulting in faster endocytosis for the vertically oriented rods to the cell membrane than for spheres with higher contact areas (3). It also is possible that some of the shape effects reported here originate from particle penetration through the glycocalyx, especially because the glycocalyx recently was shown to play a significant role in the approach of particles to endothelial cell membranes (4–6). Diffusion coefficients of small molecules in endothelial glycocalyx have been reported to be $\sim O(10^{-9})$ cm^2/s (7), which implies a diffusion coefficient of nanoparticles in the glycocalyx of $O(10^{-11})$ cm^2/s based on the Stokes–Einstein relationship. This number matches well with the experimentally measured diffusion coefficients of 200 nm polystyrene nanoparticles in human cervicovaginal mucus (8). With these diffusion coefficients, the time scales of nanoparticle diffusion through 100 nm glycocalyx would be about 10 s, a number significantly smaller than the experimental time scale, suggesting that particle approach toward HER2 receptors is not limited by the kinetics of glycocalyx penetration. Penetration through glycocalyx, however, might play an important role under flow conditions, in which the convective clearance of the particles might occur on a time scale shorter than 10 s.

It also is possible that penetration through glycocalyx depends on particle shape. Such dependence of diffusion on shape was reported recently (9). Specifically, nanorods were found to diffuse about four times faster than the spheres of comparable hydrodynamic diameter in 1% collagen gel. However, the time scales of diffusion based on the measured diffusion coefficients would be on the order of tens of milliseconds, which are 1,000–10,000-fold smaller than the time scales of our experiments, which ranged from hours to tens of hours. Thus, the kinetics of penetration or reorientation through glycocalyx are unlikely to play a role in the approach toward the membrane under the conditions reported in this study.

6. Mathematical Equation for Particle Adhesion. A semiquantitative evaluation of Eq. **1** suggests that the adhesion probability increases with the contact area between the particle and the membrane, thus explaining part of the dependence of adhesion on particle shape. However, the force of detachment, f, is also expected to depend on the particle shape. The detachment of particles from surfaces may be induced by either diffusion of particles away from the membrane or shear-induced dislodgement during washing, cell motion, or other factors that impose a relative motion between the particle and the membrane. Of these, diffusion likely plays a minimal role given the size of the particles. Precise calculation of shear-induced particle detachment in this case is challenging because the magnitude of shear forces experienced by the particles is difficult to predict. Such calculations, however, have been performed for detachment of nonspherical particles under controlled shear (10) and have shown that the detachment force changes with the aspect ratio (length/width), α (α > 1). For the sake of semiquantitative engineering analysis, we assume that this dependence can be given by the following equation:

$$f \cong \kappa\alpha^n, \qquad \textbf{[S1]}$$

where, κ is a constant and n is the power exponent, whose value may vary depending on the antibody and is not required for the semiquantitative assessment done here. The ratio of attachment probability of rods and spheres now may be described by the following equation:

$$\frac{P_{rod}}{P_{sph}} \cong \frac{(A_c)_{rod}}{(A_c)_{sph}} exp\left[-\frac{\lambda}{k_B T}\kappa(\alpha^n - 1)\right]. \qquad \textbf{[S2]}$$

The ratio of contact areas depends on the precise geometry of cell–particle contact; however, it can be assumed that this ratio increases with increasing aspect ratio because rod-shaped particles have increased surface area. Eq. **S2** may be rewritten as follows:

$$\frac{P_{rod}}{P_{sph}} \cong \alpha^m exp\left[-\frac{\lambda}{k_B T}\kappa(\alpha^n - 1)\right], \qquad \textbf{[S3]}$$

where, m is another exponent ($m > 1$) whose quantitative value is not critical for the analysis presented here. The ratio of attachment of rods and spheres may be evaluated in two limiting cases: for specific interactions ($\lambda \sim 0$) and for nonspecific interactions ($\lambda \sim \infty$). The force of detachment of antibody–antigen interaction scales with $k_B T/\lambda$. As λ approaches 0, the detachment force approaches infinity, indicating a strong bond (specific interactions). On the other hand, as the value of λ approaches ∞, the detachment force approaches zero, indicating a weak bond (nonspecific interactions).

1. Decuzzi P, Ferrari M (2008) The receptor-mediated endocytosis of nonspherical particles. *Biophys J* 94(10):3790–3797.
2. Champion JA, Mitragotri S (2006) Role of target geometry in phagocytosis. *Proc Natl Acad Sci USA* 103(13):4930–4934.
3. Vácha R, Martinez-Veracoechea FJ, Frenkel D (2011) Receptor-mediated endocytosis of nanoparticles of various shapes. *Nano Lett* 11(12):5391–5395.
4. Calderon AJ, et al. (2011) Effect of glycocalyx on drug delivery carriers targeted to endothelial cells. *Int J Transp Phenom* 12(1-2):63–75.
5. Mulivor AW, Lipowsky HH (2002) Role of glycocalyx in leukocyte-endothelial cell adhesion. *Am J Physiol Heart Circ Physiol* 283(4):H1282–H1291.
6. Agrawal NJ, Radhakrishnan R (2007) The role of glycocalyx in nanocarrier-cell adhesion investigated using a thermodynamic model and Monte Carlo simulations. *J Phys Chem C Nanomater Interfaces* 111(43):15848–15856.
7. Gao L, Lipowsky HH (2010) Composition of the endothelial glycocalyx and its relation to its thickness and diffusion of small solutes. *Microvasc Res* 80(3):394–401.
8. Tang BC, et al. (2009) Biodegradable polymer nanoparticles that rapidly penetrate the human mucus barrier. *Proc Natl Acad Sci USA* 106(46):19268–19273.
9. Chauhan VP, et al. (2011) Fluorescent nanorods and nanospheres for real-time in vivo probing of nanoparticle shape-dependent tumor penetration. *Angew Chem Int Ed Engl* 50(48):11417–11420.
10. Decuzzi P, Ferrari M (2006) The adhesive strength of non-spherical particles mediated by specific interactions. *Biomaterials* 27(30):5307–5314.

Open circles: Polystyrene rods, Filled circles: Polystyrene spheres, Filled squares: Camptothecin nanorods

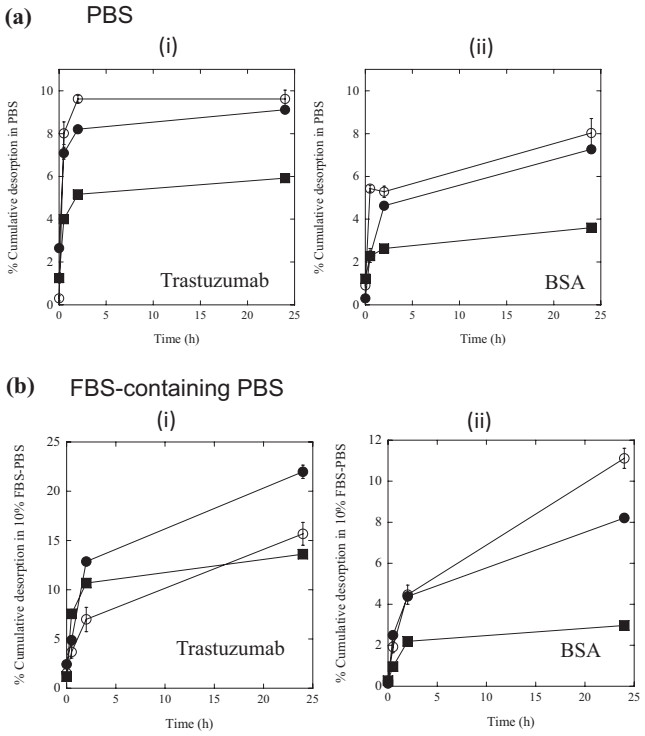

Fig. S1. Desorption kinetics of trastuzumab and BSA in (*A*) PBS and (*B*) PBS containing 10% FBS.

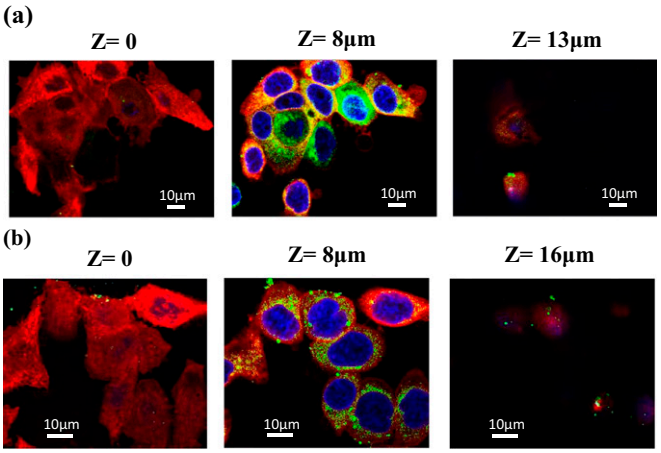

Fig. S2. Confocal images with different Z planes showing details of (*A*) trastuzumab-coated nanorod and (*B*) trastuzumab-coated nanosphere uptake by BT-474 cells. The strong green fluorescence inside cells confirms that the nanoparticles were internalized successfully. Cell boundaries were stained with CellMask Deep Red membrane stain (Invitrogen). Cell nuclei were stained with DAPI (blue).

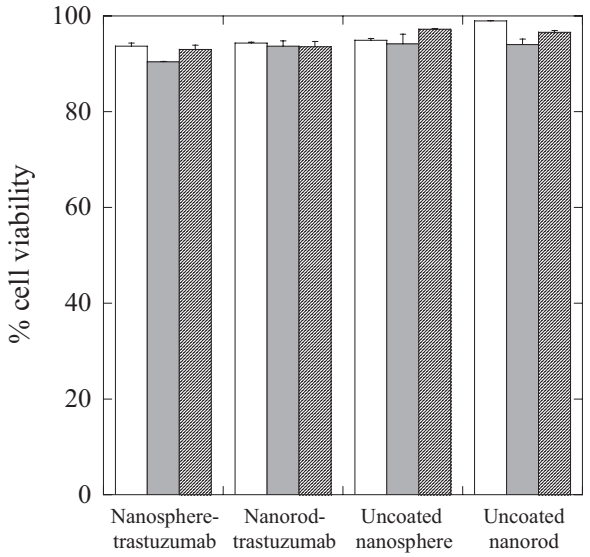

Fig. S3. Cell viability of trastuzumab-coated and uncoated nanoparticles exposed to BT-474 (open columns), SK-BR-3 (filled columns), and MDA-MB-231 cells (hatched columns). Data represent mean ± SD (n = 4).

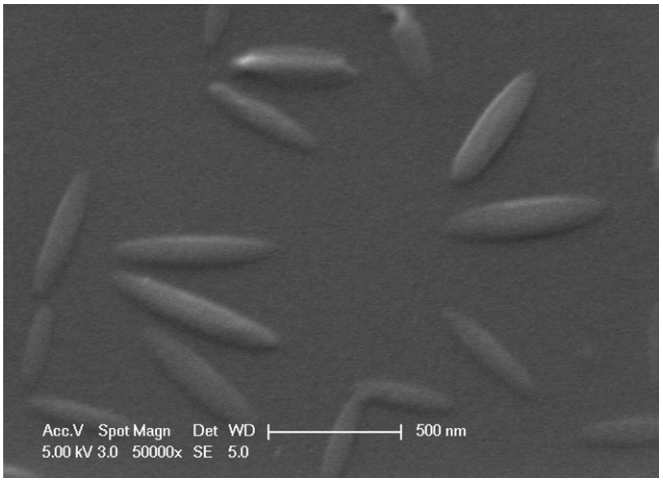

Fig. S4. PLGA nanorods prepared using film stretching.

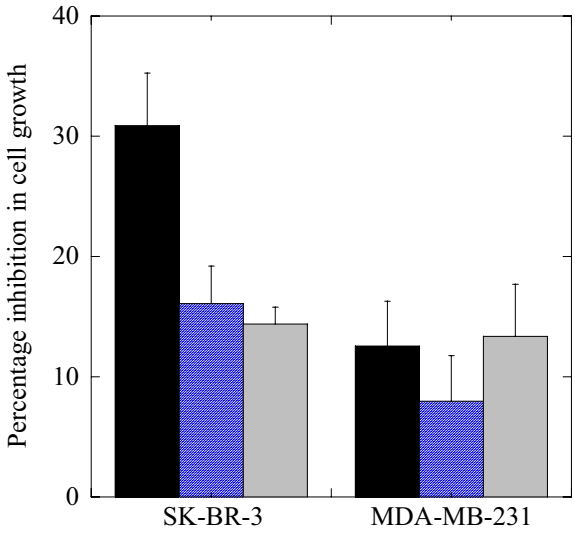

Fig. S5. Growth inhibition of SK-BR-3 and MDA-MB-231 cells using trastuzumab-coated camptothecin (black bars; concentrations of trastuzumab and camptothecin of 0.016 μg/ml and 0.1 μg/ml, respectively), BSA-coated camptothecin control (hatched bars; camptothecin concentration of 0.1 μg/ml), and trastuzumab solution alone control (gray bars; concentration of 0.016 μg/ml). Data represent mean ± SD ($n = 4$).

Table S1. Amount of adsorbed antibodies/proteins on the surfaces of nanospheres and nanorods

Nanoparticle	Mass of particles after adsorption, μg	Mass of trastuzumab adsorbed to particles, μg	Trastuzumab:particle (wt/wt) ratio	Mass of BSA adsorbed on particles, μg	BSA:particle (wt/wt) ratio
Nanosphere (200 nm)	825 ± 66	80.9 ± 11.5	0.10	35.1 ± 6.8	0.04
Nanorod (126 × 367 nm)	750 ± 120	90.3 ± 9.6	0.12	41.8 ± 13.4	0.06
Camptothecin nanorods	568.5 ± 20.8	92.3 ± 2	0.16	64.5 ± 6.5	0.11

Table S2. Surface charges on plain and targeted nanoparticles in water and cell culture medium

	Zeta potential, mV	
Nanoparticle	In water	In cell culture medium
Sphere	−20.2 ± 0.7	−9.5 ± 0.13
Rod	−22.3 ± 1.0	−9.3 ± 0.02
Sphere–trastuzumab		−5.3 ± 1.4
Rod–trastuzumab		−6.6 ± 2.6
Sphere–BSA		−7.9 ± 0.63
Rod–BSA		−8.9 ± 0.21

Table S3. Surface charges on plain and targeted camptothecin nanoparticles in water and cell culture medium

	Zeta potential, mV	
Nanoparticle	In water	In cell culture medium
Camptothecin	−33.7 ± 5.1	Not determined
Camptothecin–trastuzumab	−7.01 ± 1.4	−10.1 ± 2.3

Table S4. Binding of 300 μg/mL particles at 4 °C after 30 min incubation

Nanoparticle	Fluorescence intensity, arbitrary units
Rod–trastuzumab	119.3 ± 62.6
Sphere–trastuzumab	58.4 ± 9.4
Uncoated rod	42.7 ± 12.1
Uncoated sphere	23 ± 2.3